NOAA Technical Memorandum ERL WPL-108

A TRIPLE-BEAM ANTENNA FOR WIND-PROFILING RADAR

K. B. Earnshaw
D. C. Hogg
R. G. Strauch

Wave Propagation Laboratory
Boulder, Colorado
December 1982

noaa NATIONAL OCEANIC AND ATMOSPHERIC ADMINISTRATION / Environmental Research Laboratories

NOAA Technical Memorandum ERL WPL-108

A TRIPLE-BEAM ANTENNA FOR WIND-PROFILING RADAR

K. B. Earnshaw
D. C. Hogg
R. G. Strauch

Wave Propagation Laboratory
Boulder, Colorado
December 1982

UNITED STATES
DEPARTMENT OF COMMERCE
Malcolm Baldrige,
Secretary

NATIONAL OCEANIC AND
ATMOSPHERIC ADMINISTRATION
John V. Byrne,
Administrator

Environmental Research
Laboratories
George H. Ludwig
Director

NOTICE

Mention of a commercial company or product does not constitute an endorsement by NOAA Environmental Research Laboratories. Use for publicity or advertising purposes of information from this publication concerning proprietary products or the tests of such products is not authorized.

TABLE OF CONTENTS

A TRIPLE-BEAM ANTENNA FOR WIND-PROFILING RADAR

K.B. Earnshaw, D.C. Hogg, and R.G. Strauch
NOAA/ERL/Wave Propagation Laboratory
Boulder, Colorado 80303

ABSTRACT

An offset paraboloid with prime-focus feeds that produce three fixed beams, one directed in the zenith, and two 15° off zenith (in orthogonal planes) is discussed. The antenna is used for profiling of winds in the troposphere at UHF (915 MHz). A unique method involving tilting the reflector produces the desired beam directions, and the displacement of the feeds is only $1/\sqrt{2}$ of the conventional displacement. Measurement of the phase and amplitude of the aperture fields on a 17-GHz scale model show good agreement with ray-tracing computation. For the beam offset from boresite in the plane of symmetry, astigmatism is the first aberration observed, whereas coma is significant for a beam offset in the asymmetrical plane. Far-field patterns obtained from measurements using a near-field scanner are compared with computation.

INTRODUCTION

In recent years, measurement of wind profiles during nearly all weather conditions has been demonstrated with sensitive VHF and microwave Doppler radars.[1,2] In the optically clear atmosphere, the backscattering is from turbulent inhomogeneities in refractive index of the air. But during precipitation, and in some clouds, scattering from hydrometeors can be stronger than that from refractive turbulence of the gaseous medium, especially for the shorter radar wavelengths. The combination of a wind-measuring radar and passive microwave radiometry for measuring temperature and humidity profiles

makes possible a remote-sensing system[3] that can provide essentially continuous upper-air data.

A meteorological Doppler radar measures the mean radial motion of the scatterers in each resolution volume[4] of the beam; the scatterers follow the mean horizontal and vertical wind. Hydrometeors, if present, have a fall speed relative to the air that can be as much as 9 m s^{-1}; in general, a single Doppler radar must measure at least three radial velocity components at each resolution height to obtain the horizontal wind. Microwave radars usually obtain wind profiles by measuring the radial velocity as the antenna is rotated through a complete azimuth revolution at a suitable elevation angle.[2] Long-wavelength (VHF) radars use crossed arrays with beams pointed off zenith[5] to measure horizontal wind components. The VHF radars are primarily "clear-air" radars, i.e., they do not detect scattering from hydrometeors in non-precipitating clouds. If measurement of vertical velocities is desired, a third beam, directed toward the zenith, is added.

A remote-sensing system that continuously profiles tropospheric parameters measures the wind with a UHF (33 cm) radar designed to operate unattended in all types of weather.[3] Sensitivity requirements for clear-air operation demand a relatively large aperture, and cost and reliability dictate a mechanically fixed structure. Since a sensitive UHF radar can detect hydrometeor scattering, three antenna-beam positions are needed for the reasons discussed above. Although the three pointing directions could be chosen in a number of ways, data interpretation is simplest if one beam is directed toward the zenith and the other two sense orthogonal horizontal wind components. The beam positions used to measure horizontal wind components must be sufficiently far off zenith so that accuracy is not unduly compromised, but not so far off zenith that the height resolution at upper altitudes is degraded by an increase in the cross-beam dimensions. Wind measurement at low altitude is essential; therefore far sidelobes must be carefully controlled to minimize ground clutter that usually limits minimum radar range. Other clutter targets such as aircraft may also be detected in the sidelobes, so it is mandatory that the radiation patterns fall off as rapidly as possible. The design must therefore minimize

aperture blockage, and the feed must have essentially a Gaussian illumination with low intensity at the edges of the reflector.

1. DESIGN CONCEPT

The antenna design chosen to meet the 915-MHz wind-profiler requirements uses a fixed, offset paraboloidal reflector with feeds offset[6] in orthogonal planes. The UHF reflector is about 100 m^2 in area, resulting in a full half-power beamwidth of about 2.5°. One of the beams points toward the zenith; the other two point 15° off zenith toward the east and north. However, the unique feature is that all three feeds are offset from the focal point, and the entire structure is tilted* by 10.6° about the y axis (see Fig. 1); thus, if the reflector were illuminated by a feed at the focal point (F), the resulting beam would be directed toward the northeast at 10.6° off zenith. Figure 1 shows a plan view of the geometry of the feeds. With the antenna tilted 10.6°, this configuration generates a zenith beam (feed 1), and east- and north-pointing beams 15° off zenith (feeds 2 and 3). However, it must be emphasized that the feeds are located to produce only a 10.6° beam offset from the axis of the paraboloid, which involves an off-axis steering of only 4 beamwidths rather than 6; the zenith pointing beam is, of course, also offset 10.6° from the axis of the paraboloid. As mentioned above, in the conventional situation where the reflector is not tilted, the zenith beam would be generated by a feed at the focal point, and it would have been necessary for the east and north beams to be steered 6 beamwidths (15°). In the present configuration, all three antenna beams share some degradation caused by offsetting all three feeds. The east and north beams are identical since they are both generated by feeds offset the same amount in the $\pm y$ direction whereas the zenith beam is generated by a feed offset in the +x direction (see Fig. 1). There is some blockage from the feed and support structure for the zenith beam, but the blockage occurs where the field intensity is low.†

---

* United States Patent 4,338,608; July 6, 1982.

† The feed for the zenith beam could also be located along the -x axis, in which case the reflector would be tilted 10.6° in the other sense, resulting in no blockage; the present configuration was chosen to compact the structure.

The ratio of the focal length (f) to the diameter (D) of the offset partial paraboloid is governed by two practical constraints: choice of height of the tower that supports the feeds (see Fig. 9), and the size of the feed horns. Since the bandwidth of the radar is less than 1%, the feed horns chosen are of dual-mode[7] rather than hybrid-mode design. This feed is relatively simple to construct, and yet affords the desired quasi-Gaussian illumination. With an f/D of 0.8 (total illumination angle of 60°), the horn is required to produce illumination that tapers to about -20 dB at a 30° (half) angle to ensure low far-sidelobe radiation. A dual-mode horn with an aperture dimension of about 3λ satisfies this criterion; thus, in the full-scale 10 m antenna operating at 915 MHz, the feed-horn aperture has a dimension of about 1 m, and the focal length of the reflector is 8 m.

The performance of this design has been computed, and measurements have been made on a microwave model. The scaling ratio used is about 19:1, resulting in a model reflector of about 0.5 m, with a focal length of 0.4 m, at a test frequency of 17 GHz. All measurements discussed below pertain to the microwave model.

2. COMPUTATIONS

The optimum offset of the feed points from the focus of the partial paraboloid, for a desired beam pointing, could be determined either by measurements on a scale model or by computation. It was decided that a logical procedure was to compute the feed positions by ray-tracing and check these predictions by measurements on a scale-model antenna.

The computations take into account the amplitude and phase of the feed-horn patterns, the inverse square law relationship of the power radiating from the feed onto the reflector surface, and the phase of the reflected rays with respect to the central ray of the reflected beam. Given that the edge illumination will be about -20 dB for good far-sidelobe performance, an optimum feed point is defined as that point that produces maximum in-phase power reflected from the paraboloidal surface, measured in a local reference plane perpendicular to the desired pointing direction. Figure 2 shows an x-z plane cross

section and the ray tracing to the reference plane for the zenith beam. Total in-phase power is determined by numerical integration over the reference plane, and the final optimum feed point is found by an optimization program that locates the point giving maximum in-phase reflected power.

A. Computation of the Optimum Aim Point for the Feed Horns

A rectangular coordinate system is established in which the origin is at the vertex of the generating paraboloid of revolution; the z axis includes the focal point of the paraboloid. The boundary of the offset paraboloid is defined by x_2, x_4, and y_5, y_6 (see Fig. 3). For any given feed point, an optimum aim point is taken to be one that gives equal illumination at the paraboloid boundaries. The optimum aim point for the H (x-z) and E (y-z) planes is determined sequentially by iteration beginning with an assumed aim at the center of the reflector to achieve balanced illumination at the boundary. It is necessary to find the optimum aim point for every new feed location.

B. Computation of In-Phase Reflected Power

A reference plane, close to the paraboloid surface and perpendicular to the desired direction of the reflected beam is established (see Fig. 2); amplitude and phase are then calculated at points equally spaced over this plane. The sum of the in-phase power on the reference plane gives a measure of the quality of the feed point chosen. Calculations used in ray tracing are in the x, y, z coordinate system of the paraboloid; the equally spaced points on the reference plane are projected back onto the paraboloid. The grid points are determined by projecting the paraboloid boundaries onto the x-y plane, establishing a uniform grid of 33 x 33 points on that plane, and then projecting these points onto the paraboloid to determine the points used in ray tracing. In this method of determining points it is assumed that reflected rays all proceed in the desired aim direction. Errors in this assumption are corrected to first order by adjusting each point an amount equal to the error in pointing calculated at the intersection of the reflected ray and the reference plane.

Ray tracing is accomplished for a central incident ray which proceeds from a given feed location to its corresponding optimum aim point, and from the point of reflection to the point of intersection with the reference plane. The central incident-ray direction defines a reference vector, I_o, shown in Fig. 2, with respect to which all other incident-ray angles and amplitudes are measured. The total path of the central ray from feed location to the reference plane is a distance, L_o, against which all other ray path lengths, L, are compared, to determine relative phase.

Each incident point on the paraboloid is transformed into the coordinates of the feed horn, giving angles α_H and β_E in this coordinate system as shown in Fig. 3. Corrections are calculated for each point in the reference plane, using the source functions of amplitude, $E(\alpha, \beta)$, and phase, $\theta(\alpha, \beta)$, for the feed horn. Inverse square intensity corrections $(I/I_o)^2$ take into account attenuation from the feed point to the paraboloidal surface. In-phase power is determined from the final computed values (with "out-of-phase" power considered to be negative).

In-phase power is numerically integrated over the surface of the reference plane giving the total in-phase power for a given feed point. A search is then made for the feed location that results in the largest total in-phase power.

C. Computation of the Radiation Patterns

The optimum field over the reference plane is known at the equispaced points (as discussed in B above) because the optimum feed location has been obtained for the desired pointing direction of the beam. Computation of the far-field radiation patterns is straightforward; the same program as that used by the National Bureau of Standards for computation of fields determined experimentally (see Section 5) can be employed.

3. MEASUREMENT TECHNIQUE

The antenna laboratory of the National Bureau of Standards, Boulder, Colorado, was used to evaluate the performance of the 17 GHz model of the UHF triple-beam antenna. The phase center of the feed horn was located by mounting the horn precisely above the axis of an azimuth rotator and measuring amplitude and phase at 17.1 GHz as a function of rotation about the vertical axis. The horn is normally excited with the E vector vertical, resulting in an H-plane pattern; to obtain the E-plane pattern, the horn is simply rotated 90° about its axis. The results are discussed in Section 4.

The offset reflector and feed horn of the 17 GHz model are mounted on a support plate as sketched in Fig. 4; the plate is positioned on a table on the azimuth rotator. The assembly can be oriented in elevation as well as azimuth. The feed horn is mounted on a carriage that provides five degrees of freedom. Note that the feed support for the model is in the y-z plane (Fig. 4), whereas for the full-scale UHF antenna, the feed tower is in the x-z plane (see Fig. 9). The former configuration was necessary because of the constraints of the measurement facility. With the phase center of the feed at the focal point of the reflector, the antenna is oriented such that the z axis of the paraboloid is normal to the plane traversed by the scanning probe, also indicated in Fig. 4. The near-field amplitude and phase are then obtained by scanning the probe along the x and y axes. The near-field data are recorded on a chart recorder, and on magnetic tape for computation of the far fields (discussed in Section 5). The "on-focus" performance of the antenna serves as a reference.

For measurement of performance when the feed horn is displaced to produce beams off-boresite in the x-z (or y-z) planes, the antenna is first rotated in azimuth (or elevation) to the desired off-boresite angle (10.6°). The feed horn is then positioned and aimed, guided by the ray-tracing computation discussed in Section 2, to produce optimum near-field patterns. (Examples are shown in Figs. 6-8 of Section 5, where the distance from the reflector to the scanner is z = 76 cm.)

The separation, z, between the rotator and the scanner can be varied. Data were taken for two separations: at z = 76 cm to obtain the aperture field, and at z = 200 cm to obtain data most suitable for computation of the far fields.

4. THE FEED HORN

The dimensions of the conical dual-mode horn are shown in Fig. 4. This particular design, which incorporates an abrupt change in waveguide diameter for generating the TE_{12} mode, was provided by the Jet Propulsion Laboratory. The H-plane phase center at 17.1 GHz, located by the method discussed in the previous section, is found to be 0.63 cm behind the aperture plane. The accuracy in determining the location of the phase center is estimated to be about 2 mm. To produce the desired phase of the TE_{12} mode in the horn aperture, the 2.276-cm-diameter guide (the phasing section) is adjusted to the appropriate length.

The measured amplitude and phase patterns obtained by rotating the horn, with the phase center located on the axis of rotation, are shown by the solid line plots in Fig. 5. For a perfect spherical wave emanating from the phase center, these phase plots would remain constant during angular rotation. This behavior holds to a fair extent in Fig. 5(a), the H plane, where the phase front remains spherical within 15° over the angular range between the -10dB power levels ($\pm$20°). However, in Fig. 5(b), the E plane, for which adjustment of the relative power and phases of the two modes in the horn is most critical, the phase of the radiated field departs 20° to 30° from sphericity (where the power is at the -10 dB level); thus, the phase centers for the two planes are not exactly coincident. The illumination used in the far-field computations is shown in Fig. 5 as dashed lines; this is a Gaussian illumination.

The VSWR of the dual-mode horn, is 1.15 (return loss >23 dB). It was not considered necessary to measure the VSWR in the presence of the reflector since the offset configuration introduces negligible additional reflected power.[8]

5. COMPARISON OF MEASURED AND COMPUTED FIELDS

Three sets of measured and computed near- and far-field patterns are presented: the focused case, and the cases for beams offset in the x-z and y-z planes (see Fig. 1).

Case 1 Focused Condition

To provide a reference, and to confirm the expected performance of the feed-reflector combination, measurements were made with the phase center of the feed at the focal point. Near-field data taken along the principal axes at $z = 76$ cm, the minimum separation achievable between the antenna and the scanning probe, are shown in Figs. 6(a) and (b). The amplitude and phase computed by the ray-tracing method discussed in Section 3 for the plane $z = 10$ cm (i.e., essentially at the reflector), are shown by the dashed lines. The measurements of both amplitude and phase (at $z = 76$ cm) exhibit some rippled behavior; this is caused by interaction between the feed horn, its support system, and the probe. Near fields measured at $z = 200$ cm did not exhibit these ripples and were therefore used in computing the far fields. Agreement between measured and computed data in Figs. 6(a) and (b) is satisfactory. Between the -10 dB levels of the patterns, the measured phase agrees with the calculated values to within 10°, in spite of the interaction ripples mentioned above. In these and in the ensuing plots, increasing phase indicates increasing path length from the antenna, i.e., longer delay.

The associated measured and computed far-field patterns for the feed on the focal point are shown in Figs. 6(c) and (d). Because of the strongly tapered Gaussian illumination produced by the feed (see Fig. 5), the far-field patterns are also Gaussian in nature, and the sidelobes are low. The gain of the antenna is about 38 dB, and isotropic level is indicated by horizontal dashed lines. In the E plane, Fig. 6(d), the level of the measured far sidelobes falls somewhat below the calculations, and the first sidelobe appears as a shoulder rather than a distinct lobe. Lack of a distinct null is believed to be caused by non-coincidence of the phase centers of the feed in

the H and E planes as discussed above in Section 4. Both the measured and computed patterns in Fig. 6(c) lack perfect symmetry.

Case 2 Feed Offset in the Plane of Symmetry (x-z)

Because of practical considerations in design of the full-scale UHF antenna, beam offset in the x-z plane is achieved by moving the feed in the +x direction (rather than -x); see Fig. 1. The feed support of the 17 GHz model (not shown in Fig. 4) moves into the boundary of the aperture field, and distortion appears in the x scan; see Fig. 7(a). The y scan, Fig. 7(b), is also affected by blockage by the feed support.

The behavior of the aperture phase in Figs. 7(a) and (b) is interesting. Within the -10 dB levels, the measured and computed phase agrees to within $\pm 10°$; however, the curvature of the phase is of opposite sign in the two planes, i.e., a somewhat converging wave exists in the x-z (H) plane (Fig. 7(a)), and some divergence exists in the y-z (E) plane (Fig. 7(b)). Thus, both measurements and computations indicate that astigmatism (rather than coma) is the first aberration to appear for feed offsets in the plane of symmetry (the x-z plane).*

The principal-plane patterns of the far field, for the beam offset 10.6° from boresite in the x-z plane, are shown in Figs. 7(c) and (d). The measured values, as in Cases 1 and 3, are obtained from near-field measurements taken with the scanner at z = 200 cm. In contrast to the on-focus condition, Case 1, the levels of the measured far-field sidelobes are above the computed levels. This result is not entirely unexpected upon re-examination of Figs. 7(a) and (b), which show that distortion of the aperture field is introduced by blockage by the carriage of the feed horn. This distortion is not expected to be as severe in the full-scale UHF antenna since no sizeable (adjustable) carriage is involved. The fields fall below the isotropic level (indicated by dashed lines) at angles greater than 10° from the axis of the offset beam for both E and H planes.

---

* This behavior also appeared in computations for offset Cassegrainian configurations when one of us (DCH) was researching with M.J. Gans of Bell Laboratories.

The cross polarization was measured for this case: the characteristic peaks in cross-polarization appeared at $\pm 1.3°$ off-axis in the y direction (E plane), at a level of about -27 dB. This level is within 2 dB of the value predicted by theory for the on-focus case.[9]

Case 3 Feed Offset in the Asymmetric Plane (y-z)

Figure 8(a-d), shows the same sequence of patterns as in Cases 1 and 2, but with the feed positioned to produce a beam 10.6° (about 4 beamwidths) from boresite in the y-z plane. Since the feed and associated support system are not moved inwardly toward the aperture in this case, there is no evidence of the blockage and interaction discussed in Case 2.

The measured phase agrees with the computed values (within the -10dB levels) to within $\pm 10°$. The phase in the x scan (H plane), Fig. 8(a), is essentially flat. But for the y scan (E plane), Fig. 8(b), i.e., along the direction of feed offset, the phase exhibits an odd function in y that is characteristic of coma, and approximately obeys the equation $\psi = 6 \times 10^{-3} Y^3$, where ψ is in degrees and Y in centimeters. This behavior is in contrast to feed offset in the plane of symmetry which produced astigmatism (Case 2 above). The associated far-field patterns are shown in Figs. 8(c) and (d); in both cases, agreement between experiment and computation is very good.

The cross-polarization lobes measured in this case also attained a level of about -27 dB in the y direction, as in Case 2. Interestingly, in the y direction (E plane), the characteristic of the cross-polarization pattern is similar to the conventional pattern[9] with the feed at the focal point, but the peak level is -34 dB for the focal point feed.

The full -3 dB beamwidths (in degrees), both experimental, and computed, are given in Table 1 for all three cases.

The agreement between measured and computed beamwidths is within 10% in all cases.

Table 1.--Antenna Half-Power Beamwidths

CASE	COMPUTED		MEASURED	
	x-z plane (H)	y-z plane (E)	x-z plane (H)	y-z plane (E)
(1) Beam on boresite (focused)	2.4	2.5	2.5	2.4
(2) Beam 10.6° off in x-z plane	2.7	2.6	2.6	2.4
(3) Beam 10.6° off in y-z plane	2.6	2.7	2.6	2.6

6. CONCLUSIONS

Production of a triplet of beams, two of which constitute an orthogonal pair relative to a specified direction for a third beam, has been demonstrated to be achieved efficiently by tilting an offset paraboloid. High efficiency is obtained because of reduction in the required displacement of the feeds from the focal point by about $\sqrt{2}$, as compared with the conventional configuration. Measurements and computations show that the limiting aberrations are astigmatism and coma for beam steering in the planes of symmetry and asymmetry of the reflector, respectively. A photograph of the full-scale UHF antenna, located at the National Weather Service Forecast Office, Stapleton Airport, Denver, Colorado, is shown in Fig. 9; construction of this antenna was based upon the studies of the 17 GHz model.

ACKNOWLEDGMENT

We thank D. Bathker of the Jet Propulsion Laboratory for providing design information on the dual-mode horn, D.P. Kremer and A.G. Repjar of the National Bureau of Standards for help with the near-field measurements and computations, F.O. Guiraud and J.B. Snider of the Wave Propagation Laboratory for help with the paraboloid and feed assembly, C.G. Little for a critical reading of the manuscript, and G. Parets and C.J. Aragon of WPL for computation and plotting.

REFERENCES

1. Balsley, B.B., N. Cianos, D.T. Farley, and M.J. Baron, "Winds derived from radar measurements in the Arctic troposphere and stratosphere," J. Appl. Meteorol., 16, 1235-1239, 1977.

2. Gossard, E.E., R.B. Chadwick, K.P. Moran, R.G. Strauch, G.E. Morrison, and W.C. Campbell, "Observation of winds in clear air using an FM-CW Doppler radar," Radio Sci., 13, no. 2, 285-289, March-April 1978.

3. Hogg, D.C., "Ground-based remote sensing and profiling of the lower atmosphere using radio wavelengths," IEEE AP/S Trans. AP-28, no. 2, 281-283, March 1980.

4. Serafin, R.J., and R.G. Strauch, "Meteorological radar signal processing," Air Quality Meteorology and Atmospheric Ozone, American Society for Testing and Materials, 159-182, 1978.

5. Balsley, B.B., and W.L. Ecklund, "A portable coaxial colinear antenna," IEEE AP/S Trans., AP-20, pp. 513-516.

6. Rudge, A.W., and N.A. Adatia, "Offset-parabolic-reflector antennas: A review," Proc. IEEE, 66, no. 12, 1592-1618, December 1978.

7. Potter, P.D., "A new horn antenna with suppressed sidelobes and equal beamwidths," Microwave J., 6, 71-78, June 1963.

8. Dragone, C., and D.C. Hogg, "The radiation pattern and impedence of offset and symmetrical near-field Cassagrainian and Gregorian antennas," IEEE AP/S Trans., AP-22, no. 3, 472-475, May 1974.

9. Chu, T.S., and R.H. Turrin, "Depolarization properties of offset reflector antennas," IEEE AP/S Trans., AP-21, no. 3, 339-345, May 1973.

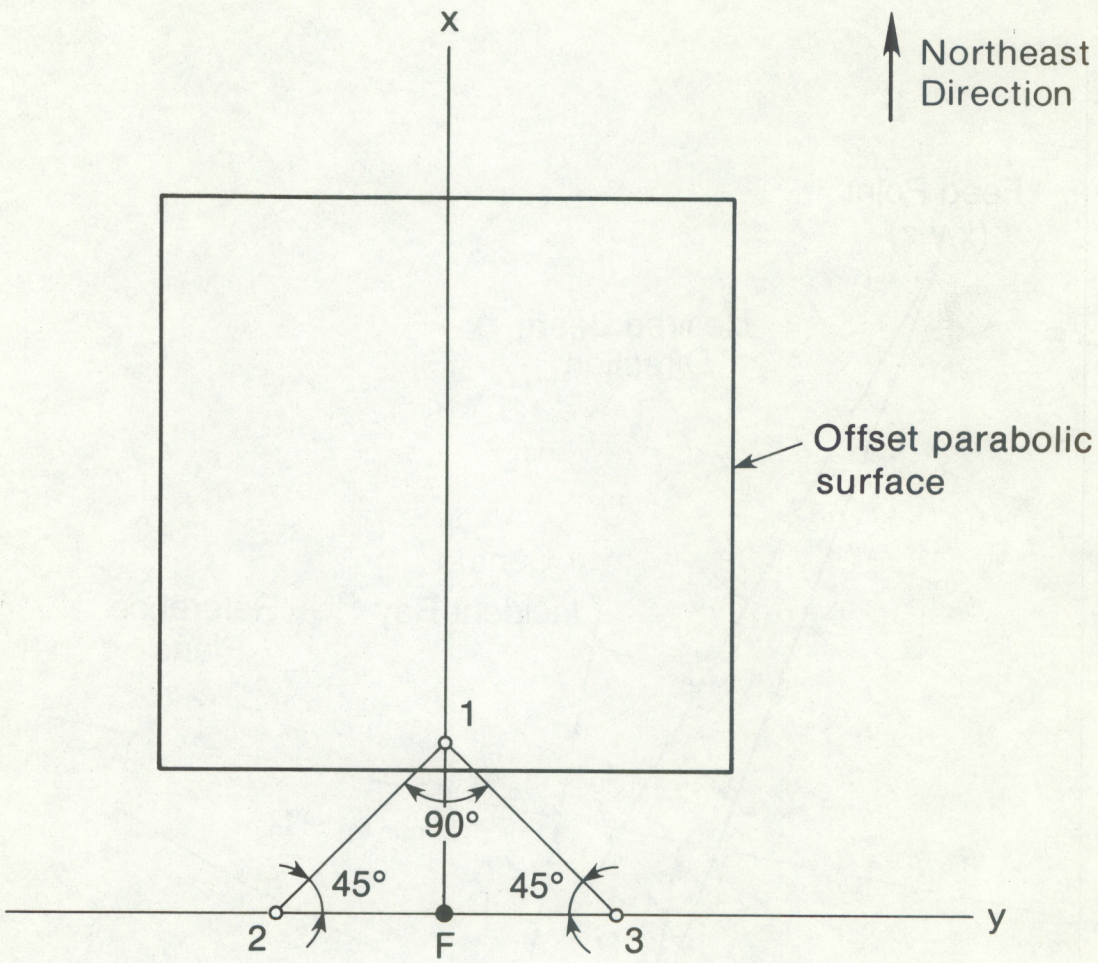

Figure 1. Horizontal plan view of offset paraboloidal system showing the coordinate system used, the position of the focus, F, and the position of the three displaced feeds, each located to produce a beam 10.6° offset from the paraboloidal axis. The paraboloidal surface is tilted so that the axis of symmetry of the generating paraboloid of revolution is 10.6° from the zenith toward the northeast. This tilting brings the beam from feed 1 into the zenith; feeds 2 and 3 then produce beams inclined 15° from the zenith toward the east and north, respectively.

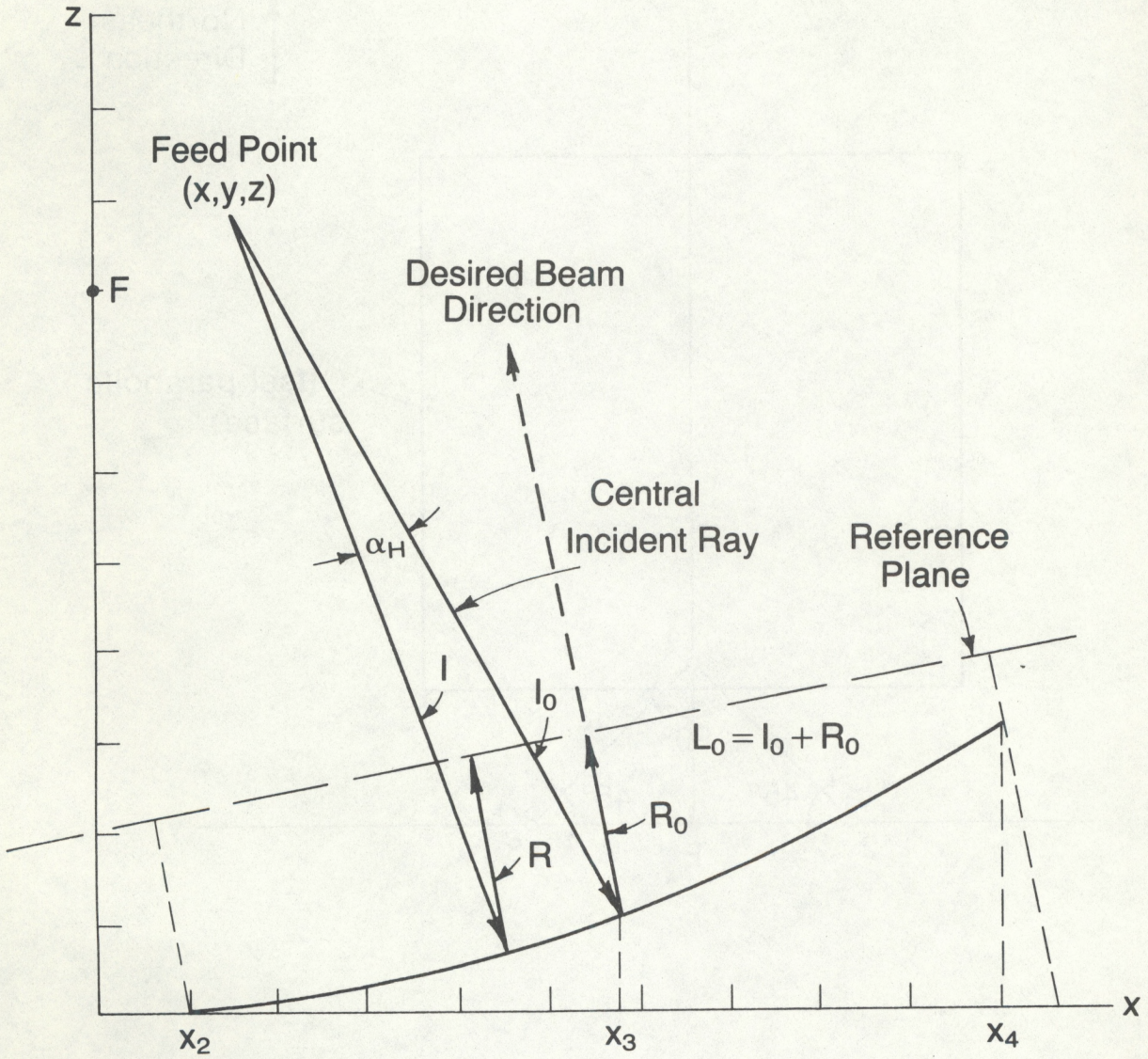

Figure 2. Cross-section in the x-z (H) plane showing ray tracing for the zenith beam, and position of the reference plane with respect to the paraboloid.

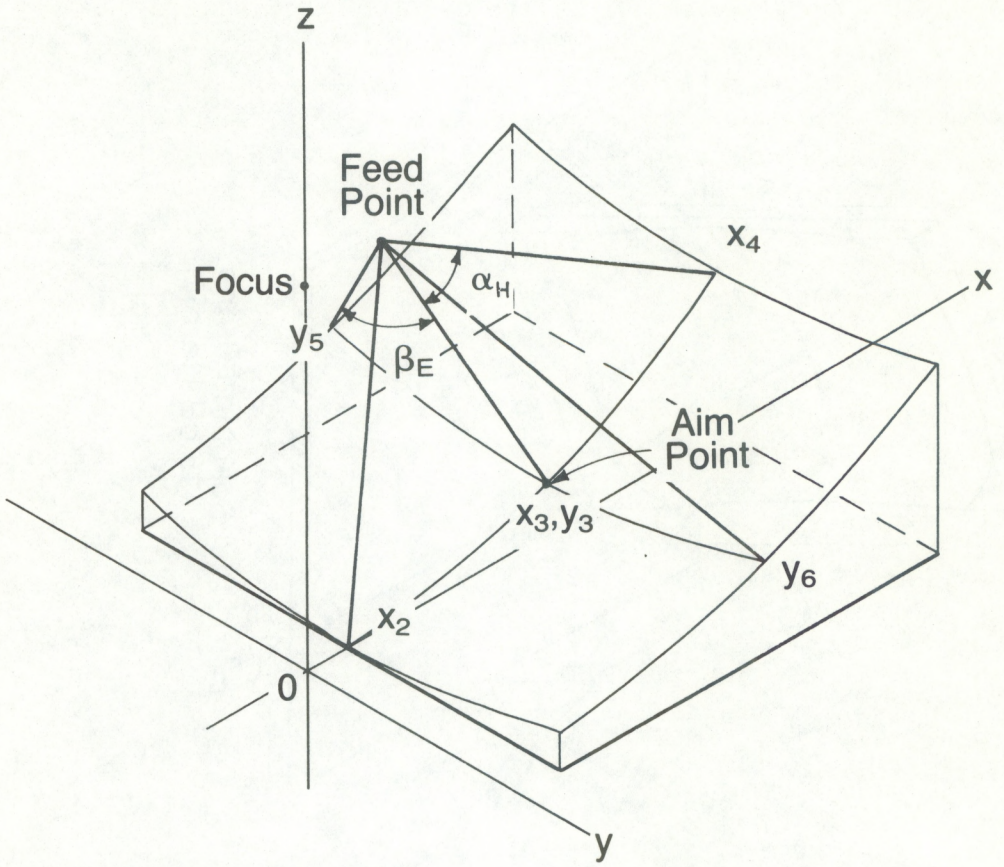

Figure 3. Coordinate system for calculation of correct aim point and ray tracing. The maximum subtended angles in the H (x-z) and E (y-z) planes, α_H and β_E, are also shown.

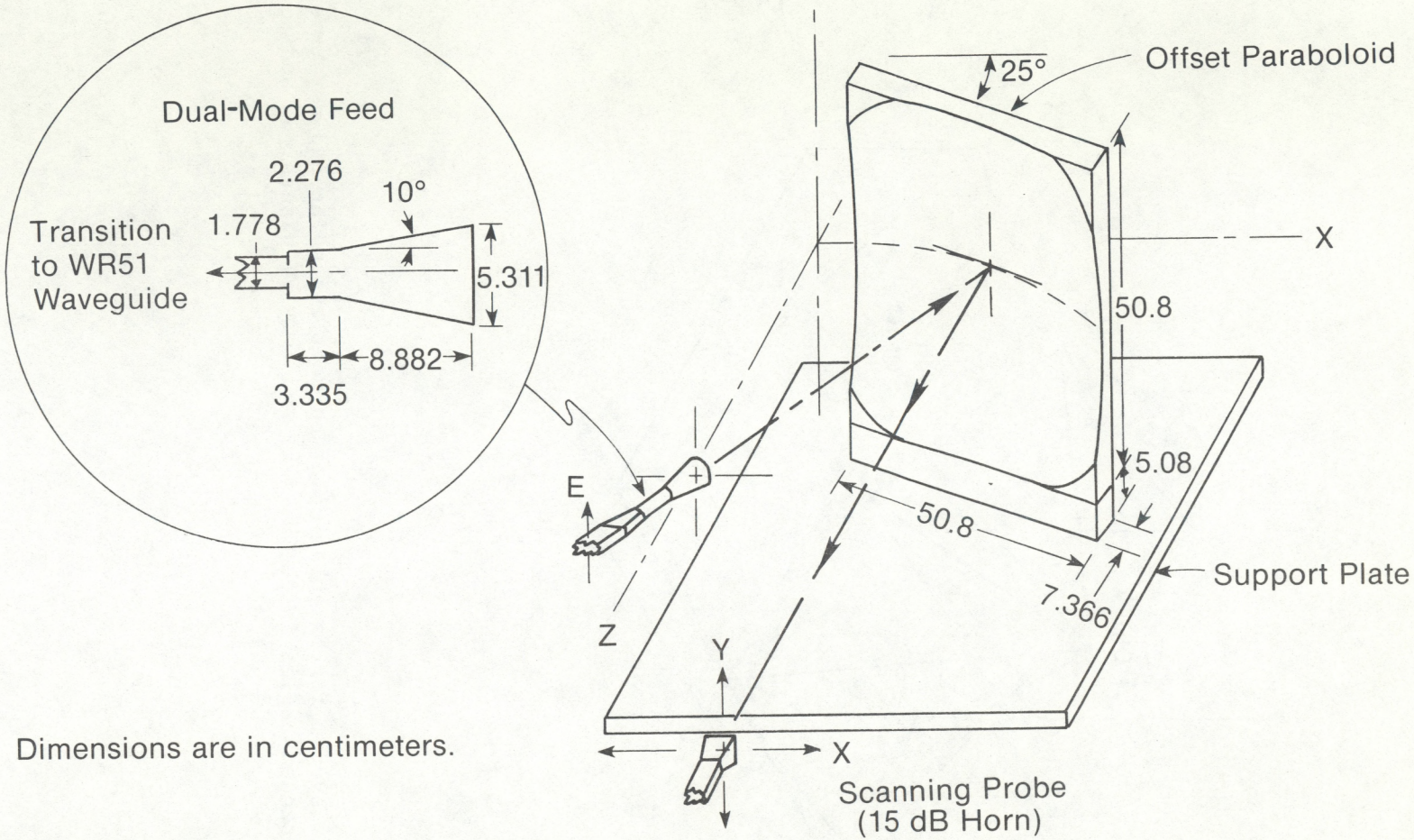

Figure 4. Experimental configuration of the offset reflector and feed horn (mounted on a support plate) for measurement of the near fields.

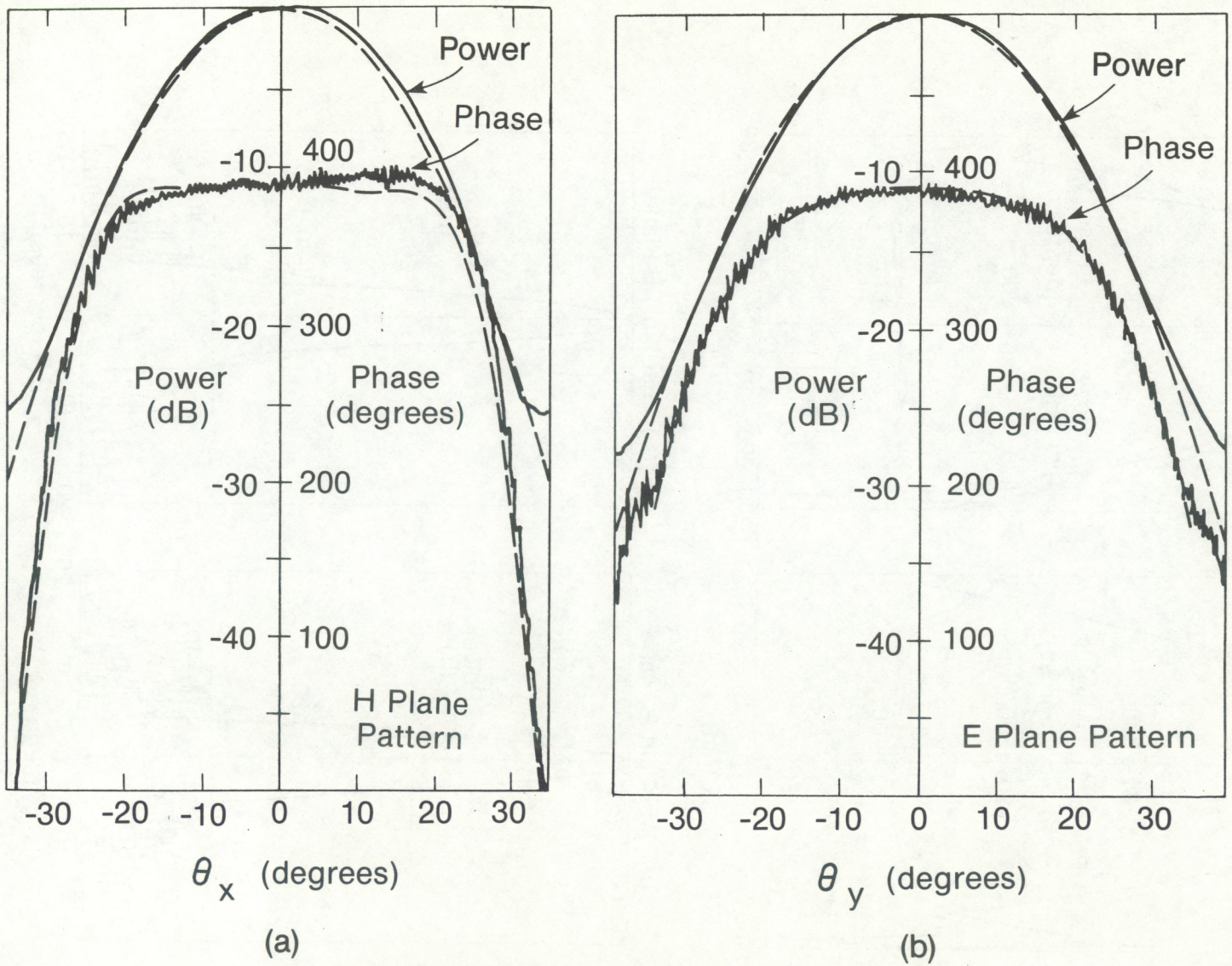

Figure 5. Radiation patterns of the feed horn. ——— measured ----- theoretical. The phase ripples are caused by horn-probe interaction.

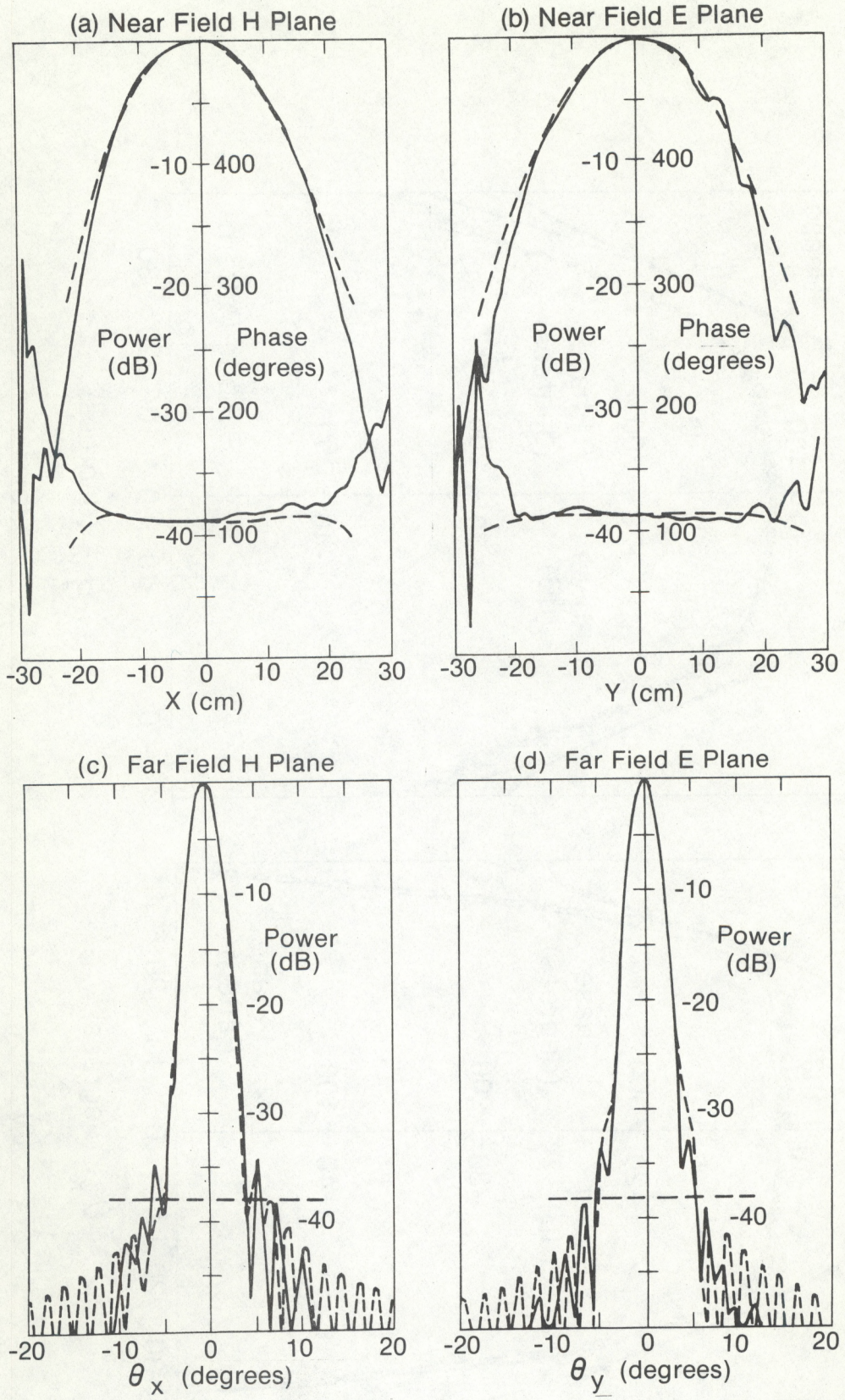

Figure 6. Measured (in the z = 76 cm plane) and calculated (in the z = 10 cm plane) near-field patterns with the phase center of the feed near (0.5, 0, 40), the focal point; the aim point on the reflector is (x = 28.2, y = 0); (a), H plane; (b), E plane; (c) and (d) are the measured and calculated far-field patterns for the H and E planes. Measured patterns are solid lines and calculated are dashed.

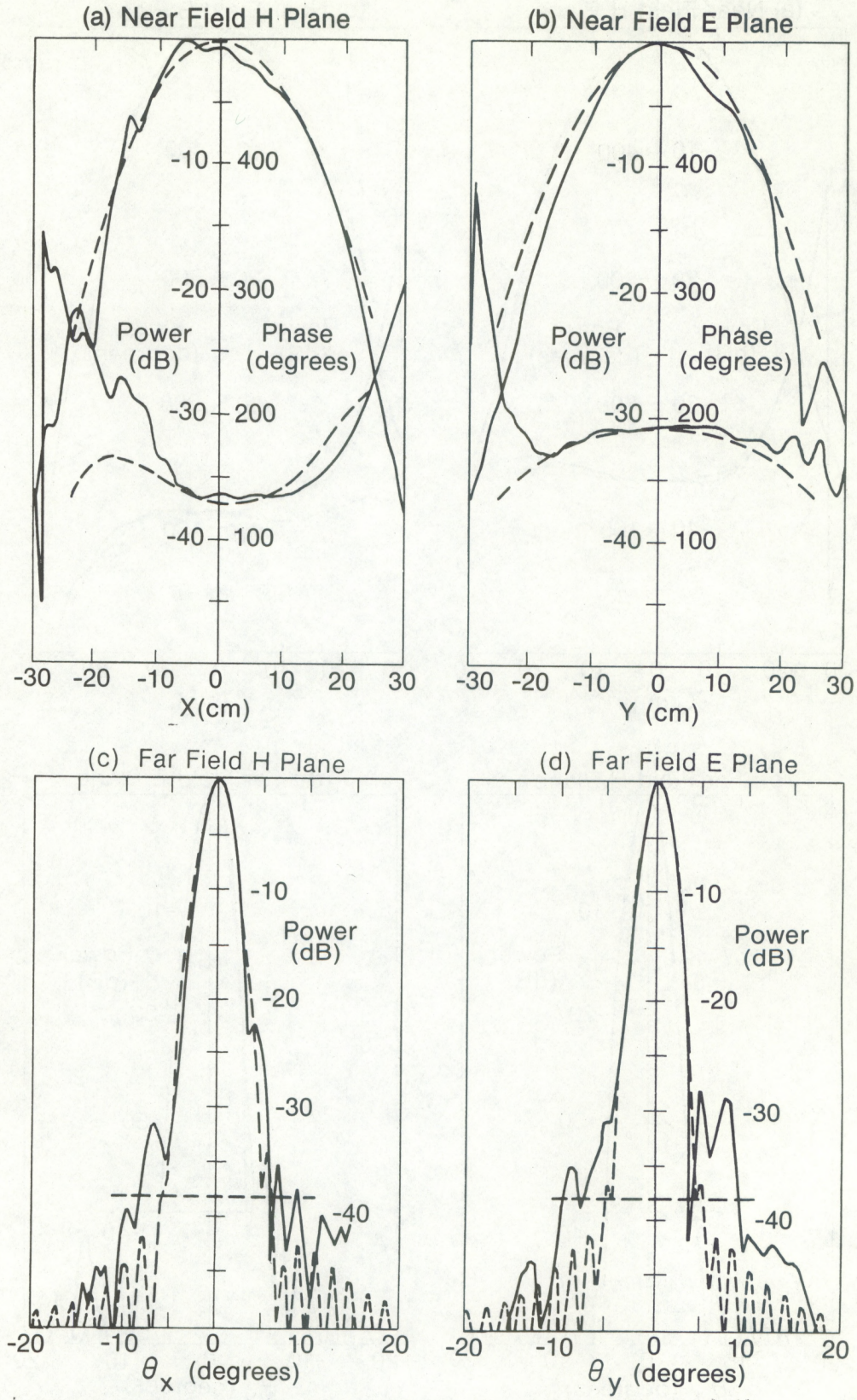

Figure 7. Measured (in the z = 76 cm plane) and calculated (in the z = 10 cm plane) near-field patterns with the phase center of the feed displaced (7.8, 0, 44.3) to produce a far-field beam 10.6° off-boresite in the x-z plane; the aim point on the reflector is (x = 29.8, y = 0); (a), H plane; (b) E plane; (c) and (d) are the measured and calculated far-field patterns for the H and E planes. Measured patterns are solid lines and calculated are dashed.

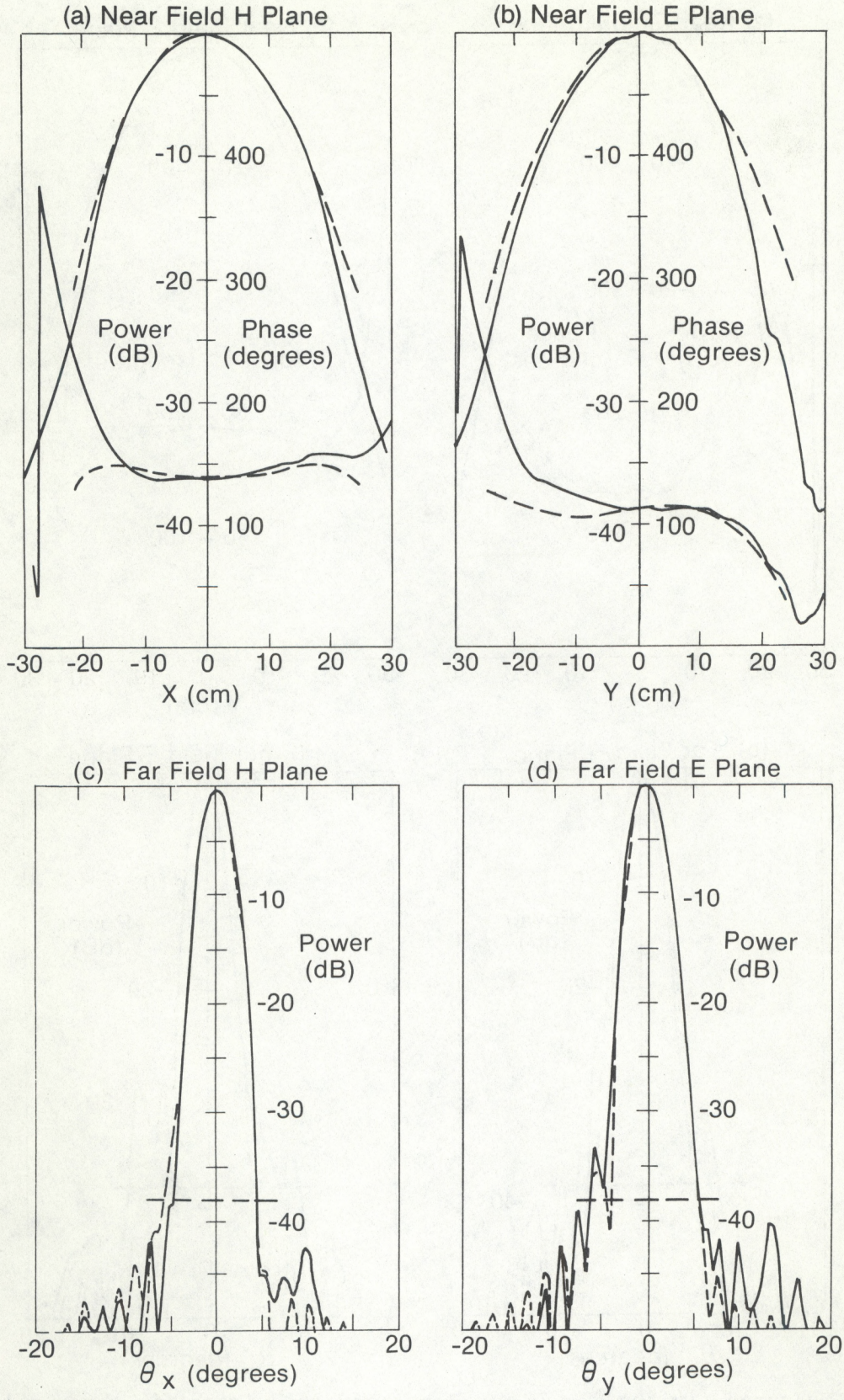

Figure 8. Measured (in the z = 76 cm plane) and calculated (in the z = 10 cm plane) near-field patterns with the phase center of the feed displaced (0.6, 8.4, 39.6) to produce a far-field beam 10.6° off boresite in the y-z plane; the aim point on the reflector is (x = 28.2, y = 1.7); (a), H plane; (b), E plane; (c) and (d) are the measured and calculated far-field patterns for the H and E planes. Measured patterns are solid lines and calculated are dashed.

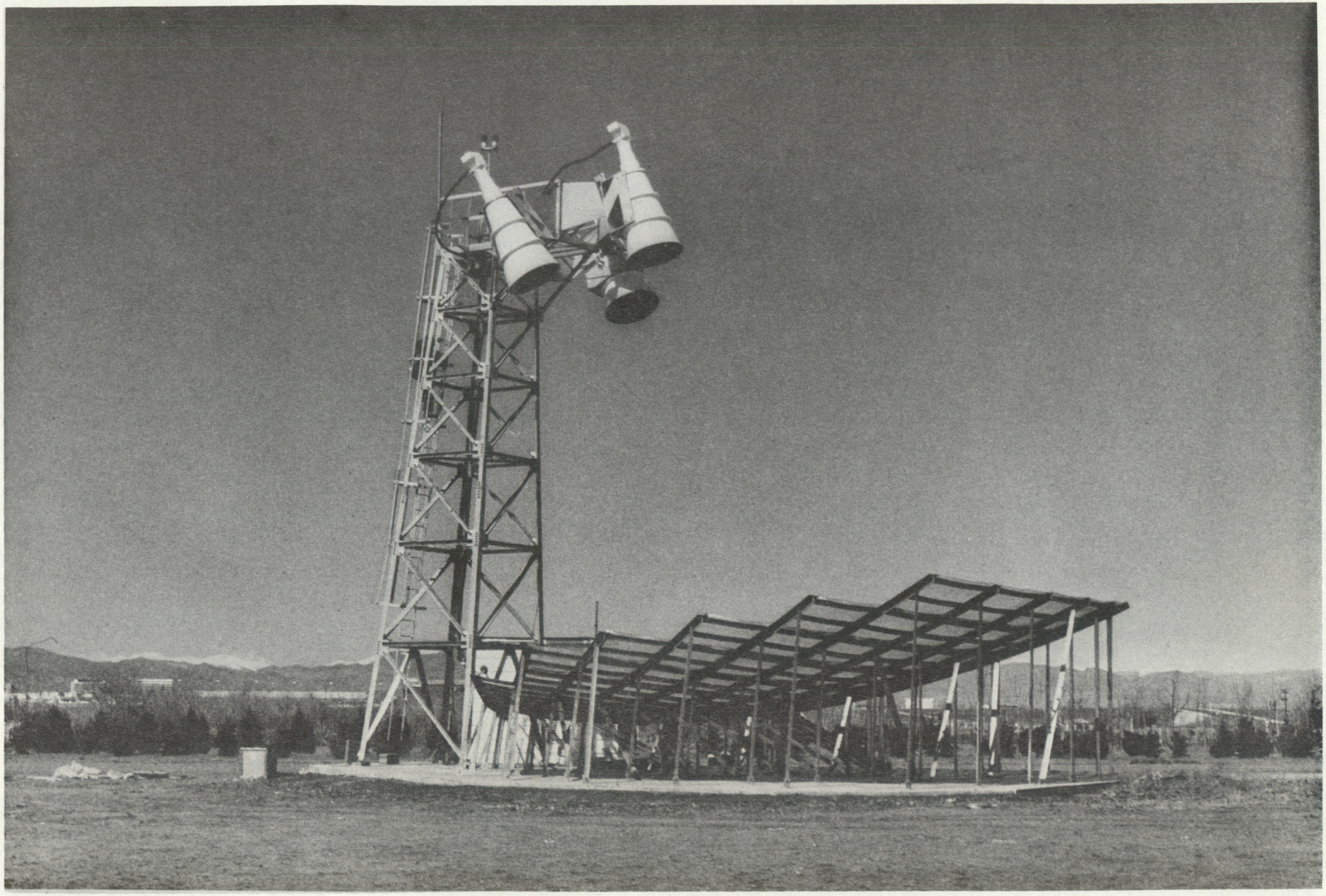

Figure 9. Photograph of the full-scale triple-beam antenna operating at 915 MHz.